Pharm Res (2013) 30:1065–1076
DOI 10.1007/s11095-012-0943-x

RESEARCH PAPER

Critical Solvent Properties Affecting the Particle Formation Process and Characteristics of Celecoxib-Loaded PLGA Microparticles *via* Spray-Drying

Feng Wan • Adam Bohr • Morten Jonas Maltesen • Simon Bjerregaard • Camilla Foged • Jukka Rantanen • Mingshi Yang

Received: 16 August 2012 / Accepted: 19 November 2012 / Published online: 11 December 2012

ABSTRACT

Purpose It is imperative to understand the particle formation mechanisms when designing advanced nano/microparticulate drug delivery systems. We investigated how the solvent power and volatility influence the texture and surface chemistry of celecoxib-loaded poly (lactic-co-glycolic acid) (PLGA) microparticles prepared by spray-drying.

Methods Binary mixtures of acetone and methanol at different molar ratios were applied to dissolve celecoxib and PLGA prior to spray-drying. The resulting microparticles were characterized with respect to morphology, texture, surface chemistry, solid state properties and drug release profile. The evaporation profiles of the feed solutions were investigated using thermogravimetric analysis (TGA).

Results Spherical PLGA microparticles were obtained, irrespectively of the solvent composition. The particle size and surface chemistry were highly dependent on the solvent power of the feed solution. An obvious burst release was observed for the microparticles prepared by the feed solutions with the highest amount of poor solvent for PLGA. TGA analysis revealed distinct drying kinetics for the binary mixtures.

Conclusions The particle formation process is mainly governed by the PLGA precipitation rate, which is solvent-dependent, and the migration rate of celecoxib molecules during drying. The texture and surface chemistry of the spray-dried PLGA microparticles can therefore be tailored by adjusting the solvent composition.

KEY WORDS celecoxib · microparticles · particle formation · poly (lactic-co-glycolic acid) · spray drying

INTRODUCTION

A significant number of solid dosage forms developed by the pharmaceutical and biotech industries are based on microparticles because they have shown to be effective in i) enhancing drug targeting specificity, ii) lowering systemic drug toxicity, iii) improving drug absorption rates, and iv) providing protection for pharmaceuticals against chemical and enzymatic degradation (1). In addition, they can be tailored to a wide variety of administration routes, including parenteral, oral, nasal and pulmonary delivery (1–5).

Several technologies have been used to design and fabricate microparticles with the aforementioned functionalities, including double emulsion solvent evaporation methods (6), phase separation techniques (7), spray-drying (8–13), spray-freeze-drying (8,9,14–16), supercritical fluid technology (8,9,17,18) and electrospray-drying (19–21). Among them, spray-drying may be the most preferred technology in the pharmaceutical industry for such purpose because it is a fast and continuous one-step process. Moreover, it is the most

Feng Wan and Adam Bohr contributed equally to the manuscript.

F. Wan • A. Bohr • C. Foged • J. Rantanen • M. Yang (✉)
Department of Pharmacy, Faculty of Health and Medical Sciences
University of Copenhagen Universitetsparken 2
2100 Copenhagen Ø, Denmark
e-mail: mingshi.yang@sund.ku.dk

A. Bohr
Department of Mechanical Engineering, University College London
Torrington Place
London WC1E 7JE, UK

M. J. Maltesen
Biopharma Application Development, Novozymes Biopharma A/S
Krogshoejvej 36
2880 Bagsvaerd, Denmark

S. Bjerregaard
Preformulation and Delivery/Oral Protein Delivery
Diabetes Research Unit, Novo Nordisk A/S, Måløv Byvej 200
2760 Måløv, Denmark

feasible technique among the aforementioned methods due to the possibility for an industrial scale production.

In line with the concept of Quality-by-Design (QbD) approach, numerous attempts have been made to define, understand and control formulation and process variables to assure the quality attributes of the final spray-dried product. It is of crucial importance to understand the mechanisms behind the particle formation process during spray-drying. However, most particle engineering approaches have largely been based on characterization of the final product, followed by adjustment of the composition of the formulation and/or optimizing the drying process parameters to meet the specifications (22–26).

To date, a few mathematical models have been developed to describe the particle formation process during spray-drying. One of the most commonly used models is the constant evaporation rate model, which has been discussed in literature (1,27–30). The evaporation rate constant, κ, is defined according to Eq. 1:

$$d^2(t) = d_0^2 - \kappa\, t \tag{1}$$

where d_0 is the initial droplet diameter, t is the time and $d(t)$ is the droplet diameter at time t. The droplet drying time (τ_D) can be calculated from Eq. 2:

$$\tau_D = d_0^2/\kappa \tag{2}$$

The Peclet number (Pe) described in Eq. 3 is an important parameter in the spray-drying process, which can be used to predict the particle formation process and the resulting particle properties:

$$Pe_i = \kappa/8D_i \tag{3}$$

where Pe is a dimensionless number and D is the diffusion coefficient.

The surface enrichment (Ei) [the surface concentration of component i ($C_{s,i}$) relative to its average concentration in the droplet ($C_{m,i}$)] and the time required for a component to reach saturation at the surface of droplet ($\tau_{sat,\ i}$) can be approximated by the Eqs. (4) and (5), respectively.

$$E_i = C_{s,i}/C_{m,i} = 1 + Pe_i/5 + Pe_i^2/100 - Pe_i^3/4000 \tag{4}$$

$$\tau_{sat,\ i} = \tau_D\left(1 - \left(S_{0,i}Ei\right)^{2/3}\right) \tag{5}$$

where $S_{0,i}$ is defined as the ratio between the initial concentration of the components in the feed solution ($C_{0,i}$) and its saturation concentration ($C_{sat,\ i}$).

As indicated by Eqs. 1–5, Pe depends on the drying rate (κ) and the diffusion coefficient (D_i) of the solutes, as well as the solubility of the solutes and the initial concentration of the solution, which are the key factors influencing the solidification of the solutes and the particle formation process. When $Pe \leq 1$, the diffusional velocity of the solute in a droplet is faster or in the same order of magnitude as the solvent recession rate at the droplet surface (drying rate) and consequently, the radial concentration profile of the solute is predicted to be flat. For such small Pe with a large solute solubility, precipitation of the solutes is expected to appear at a late stage of the evaporation process, which leads to condensed particles with a relatively homogeneous distribution of solutes in the resulting particles. For $Pe > 1$, the recession of the droplet surface is faster compared to the diffusion of the solute molecules. Therefore, the solutes tend to accumulate at the surface and precipitate at the surface, resulting in shell formation. Particles formed under such circumstances typically have voids and a lower density (1,27,30). Hence, by characterizing the solubility, the diffusion rate of the solutes and the drying rate, these models can to some extent be used to predict the particle formation process.

However, these models are based on the assumption of a constant drying rate during the spray-drying process and without considering the existence of solvent-solvent and solute-solute interactions during drying. Their use may therefore be restricted to relatively simple systems composed of a single solute component and/or a single solvent system. When multiple solutes and solvents are applied, describing the shrinkage of the droplets and the mobility (diffusion) of the solutes in the droplet becomes much more complicated due to the existence of both solvent-solvent and solute-solute interactions during drying (the solutes may have different solubilities and diffusion coefficients in different solvents). Thus, a more thorough investigation of the interplay between solutes and solvents during the particle formation process is required for rational particle engineering *via* spray-drying.

The influence of the solvent composition on the particle morphological characteristics (23), physical stability (31) and drug release profile (32) of spray-dried microparticles has been studied with an emphasis on characterizing the resulting microparticles and investigating the formulation and/or process parameters that influence the final product attributes. However, less emphasis has been given to understanding the effect of critical solvent properties (e.g. solvent power and volatility) on the particle formation process and the resulting particles characteristics, such as the inner texture and surface chemistry, and their effect on the drug release profile. In the present study, we aimed to investigate how the interplay between the solvent power and the drying rate influences the formation and physicochemical characteristics of celecoxib-loaded PLGA microparticles prepared by spray-drying. PLGA was chosen because it is one of the most extensively used polymers for controlled-release formulations (33). Celecoxib, a selective COX-2 inhibitor, was used as a poorly water-soluble model drug (solubility approximately 5 μg/ml in water) (34). Various solvent systems

composed of acetone (ACE) or binary mixtures of ACE and methanol (MeOH) were employed to vary the solvent power and the drying rate systematically. ACE and MeOH were selected to form the solvent mixtures because they are a good solvent and a poor solvent for PLGA, respectively. By using different compositions of these two solvents we intended to understand how anti-solvent precipitation during the drying process influences the microscopic structure of the spray-dried PLGA microparticles. In addition, ACE and MeOH have different boiling points, indicating the different evaporation rates with acetone evaporating faster. The binary mixtures of ACE and MeOH were also employed to study the impact of the drying rate on the process of particle formation and particle characteristics. The spray-dried microparticles were characterized by applying a number of advanced techniques to the analysis of the morphology, inner structure, surface chemistry, solid state properties and drug release rates.

MATERIALS AND METHODS

Materials

Celecoxib was purchased from Dr. Reddy [99.6%, Hyderabad, India (M_w=381.38 g/mol)]. PLGA, acid terminated, 50:50, M_w=24,000–38,000, [$(C_6H_8O_4)_X(C_4H_4O_4)_Y$]n), acetone (ACE, 99.9% HPLC grade) and methanol (MeOH, 99.9% HPLC grade) were purchased from Sigma–Aldrich (Poole, UK).

Methods

Determination of Evaporation Rates

The evaporation rates of the pure solvents and the binary feed solutions used in the spray-drying process were mimicked and estimated by thermogravimetric analysis (TGA), using a TGA 7 (Perkin Elmer, Waltham, Massachusetts, USA). Briefly, approximately 20 µl solvent or feed solution was transferred into a platinum pan, placed in the sample holder and enclosed inside the temperature-controlled furnace constantly purged with nitrogen at a flow rate of 20 ml/min. The temperature was kept constant at 30°C to mimic the outlet temperature during the spray-drying process. The weight loss was recorded as a function of time.

Particle Preparation by Spray-Drying

PLGA microparticles loaded with celecoxib were prepared using a Büchi B-290 spray dryer (Büchi Labortechnik AG, Postfach, Switzerland) equipped with an inert loop B-295 (Büchi Labortechnik AG). All samples were prepared at identical drying conditions (inlet temperature: 45°C; outlet temperature: 30°C; drying air flow rate: 22.5 m^3/h; atomizing air flow rate: 742 L/h and feed flow rate: 3 ml/min). The gentle drying conditions, especially the relatively low outlet temperature, were chosen due to the low glass transition temperatures of PLGA (45°C) and celecoxib (51°C), respectively (34,35).

Particle Size and Morphology

The morphology and particle size of the spray-dried particles were visually examined using a Zeiss Ultra55 scanning electron microscope (SEM, Carl Zeiss, Denmark). The samples were transferred onto sticky carbon tape and mounted on metallic stubs, followed by sputter coating with a 5 nm thick layer of gold to make the surfaces conductive. The specimens were then imaged at an accelerating voltage of 3 kV with a 30 µm aperture. The particle sizes and distributions were measured by conventional image analysis using a software (Image J, NIH, USA): The Martin's diameter of 100–150 randomly selected particles was determined in a fixed direction (left to right) from the field of view of the SEM images. The size data were expressed as D_{10}, D_{50}, D_{90}, which are diameters at 10%, 50%, and 90% cumulative number, respectively. The broadness of the size distribution, known as the span, equals $(D_{90}- D_{10})/D_{50}$.

Focused Ion Beam-Scanning Electron Microscopy (FIB-SEM)

A Zeiss 1540 XB Cross Beam Scanning Electron Microscope (Carl Zeiss, Denmark) equipped with a 30 kVGa^+ FIB-gun was used to investigate the inner structure of the spray-dried microparticles. Briefly, an automated FIB-SEM slice-and-view procedure was used for characterization. The ion beam removes thin sections of the particles, pausing the milling process at a predetermined time interval, and an image of the newly exposed area is saved. The slice-and-view process continued through the particle, exposing the internal structure. The resulting image stack was post processed in Image J (NIH, USA) using StackReg for alignment (translation in x, y only).

Differential Scanning Calorimetry (DSC) and Thermogravimetric Analysis (TGA)

DSC measurements were carried out using a PerkinElmer series DSC 7 thermal analysis system (PerkinElmer Ltd., UK). Samples (5–10 mg) were crimped and sealed in aluminum DSC pans with vented lids, which were placed in sample cells under nitrogen. Samples were heated from 25 to 200°C at a scanning rate of 10°C/min. The bulk samples were analyzed using a TGA 7 (Perkin Elmer, Waltham, Massachusetts, USA) under a nitrogen purge of 20 ml/

min. Samples (ca. 5–10 mg) were loaded onto an open platinum pan and heated from 20 to 120°C at a scan rate of 10°C/min.

X-ray Powder Diffraction (XRPD)

The X-Ray powder diffraction spectra were recorded on a PANalytical X'Pert PRO MPD (PW3040/60, Philips, Netherlands) using a copper (Cu) anode for radiation with λ=1.542 Å, 45 kV and 40 mA. The samples were transferred onto a silicium plate fitted in a sample holder. The samples were measured from 5° to 40° 2θ with a step size of 0.053° and 0.025° per second.

Drug Entrapment Efficiency

The drug entrapment efficiency (EE) was measured by evaluating the total amount of drug in the collected samples. Samples of 10–20 mg microspheres were accurately weighed, dissolved in acetonitrile (10 ml) and agitated for 1 h. This solution was then diluted 1:10 in acetonitrile:water (20:80, v/v) and centrifuged at 3,000×rpm for 10 min. The drug content in the supernatant was analyzed using an HPLC unit with a P680 pump, an ASI 100 sample injector and UVD340U detector (Dionex, Idstein, Germany) equipped with a Kromasil 126 column (Kromasil, Partille, Sweden). A mobile phase of acetonitrile:water (60:40, v/v) was used at a flow rate of 0.5 ml/min, the injection volume was 10 µl, and the samples were detected at wavelength 230 nm and a run time of approximately 15 min. A calibration curve was generated from reference celecoxib solutions ranging from 0.5 to 50 µg/ml, and a good linear correlation was achieved in the entire range. The drug entrapment efficiency was then determined according to Eq. 6:

$$\text{EE}\,\% = 100 \times \text{Mass of drug loaded in particles} / \text{Mass of drug processed} \quad (6)$$

The drug entrapment efficiency was taken into account when analyzing the drug release data, and the release data was corrected by linear scaling of each data point.

Drug Release Behavior in Vitro

The *in vitro* drug release behavior was investigated using the USP paddle method. Briefly, celecoxib-loaded microspheres were suspended in a release medium of phosphate-buffered saline (PBS) containing 1.5% (w/v) sodiumlaurylsulphate (SLS) to ensure sink conditions. Dissolution studies were performed using a Sotax AT7 dissolution station (Sotax, Allschwil, Switzerland) equipped with a USP II (paddle) apparatus and 1,000 ml glass vessels. Samples were withdrawn through a 2.7 µm glass microfiber filters (Whatman Ltd, Oxon, England) using a Biolab/Gilson GX-271 autosampler (Biolab, Gloucestershire, UK). Samples were weighed (10–20 mg) and placed in 500 ml release medium at a paddle rotation of 50 rpm at 37°C. Samples of 5 ml were taken at each time point and analyzed by HPLC as described above. A minimum of four experiments were performed for each microparticles formulations, and the cumulative drug release profiles were constructed.

X-ray Photoelectron Spectroscopy (XPS)

Particles on glass slides were analyzed by XPS using a K-Alpha (Thermo Scientific, Denmark) equipped with a monochromated AlKα X-ray source with energy of 1486.6 eV. Wide energy survey scans (0–1,350 eV binding energy) were acquired with pass energy of 200 eV and step size of 1.0 eV. Additional high resolution spectra of carbon (C1s), oxygen (O1s) and silicon (Si2p) were acquired using pass energy of 25 eV and a step size of 0.1 eV. The angle between the sample surface and the analyzer (take-off angle) was 90°. Charge compensation was accomplished with a dual beam flood gun. An X-ray spot size of 200 µm was used for the spray-dried particles due to the inhomogeneous coverage. The drug content (in weight %) was determined by rationing the detected amount of fluorine in the sample to the amount of fluorine in celecoxib.

Statistics

Measurements were performed in triplicate, unless otherwise stated. Values are given as means±SD. Statistically significant differences were assessed by an analysis of variance (ANOVA) at a 0.05 significance level, followed by the *t*-test (Excel, Microsoft, USA).

RESULTS

Measurement of Evaporation Rates

The evaporation profiles of the solvents (without celecoxib and PLGA) showed reversed S-shapes representing three distinct drying phases (Fig. 1a) i.e. an initial slowly declining evaporation rate, a fast declining evaporation rate and a slowly declining evaporation rate. During the first phase, a rapid loss of solvent mass took place, and the evaporation rate was mainly governed by the affinity between the solvent molecules. In the second phase, the evaporation rate decreased rapidly, indicating that the major part of the solvents has evaporated. In the third drying phase, the rate of

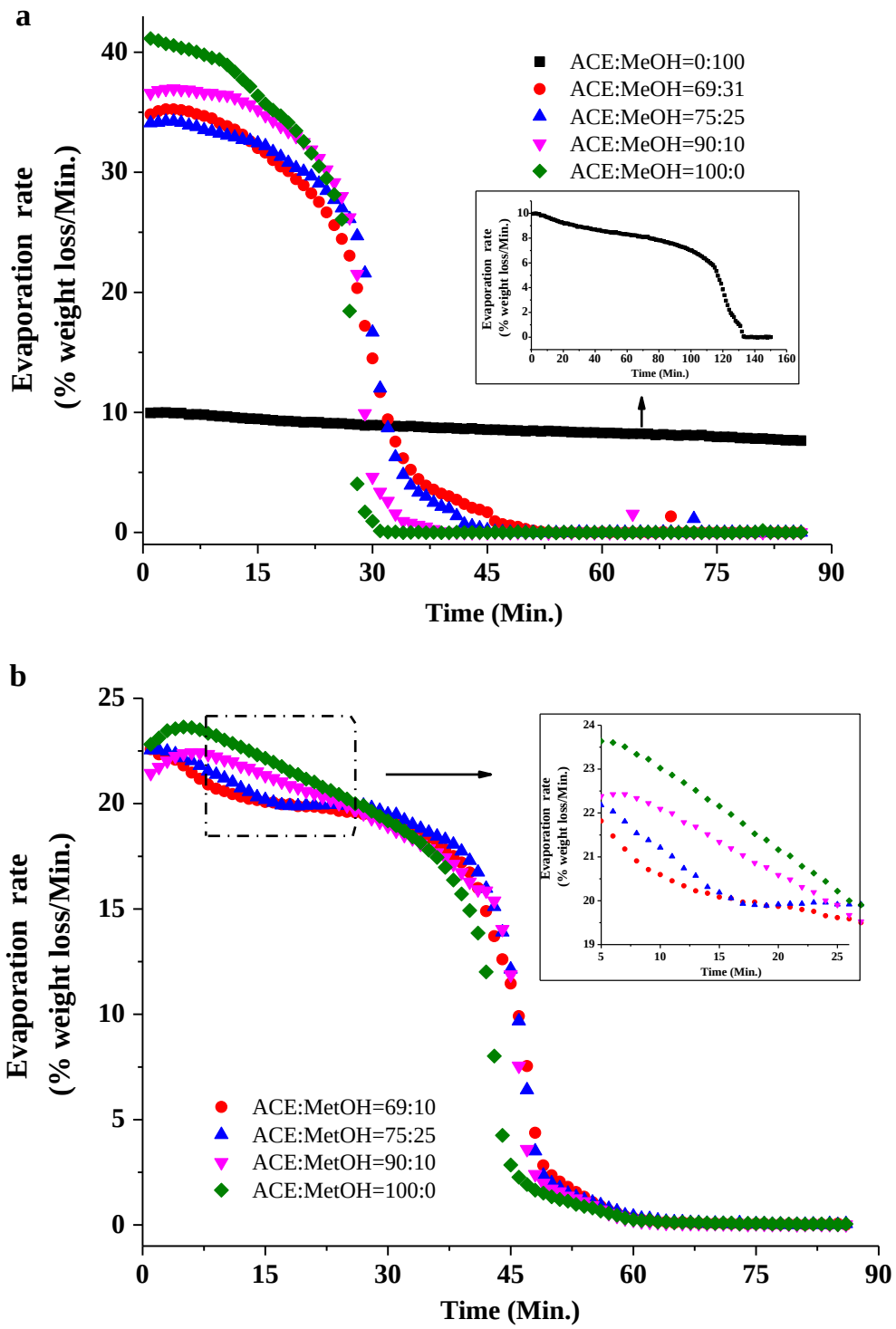

Fig. 1 Estimation of the evaporation rates of the pure solvents (**a**) and the feed solutions (**b**). Results denote average value (n=3)

mass loss of residual solvents decreases further because less solvent was available for evaporation.

The evaporation profiles of the solvents were significantly changed when PLGA and celecoxib were added to the solvent systems. Four drying phases were observed for the two solvent systems at ACE:MeOH molar ratios of 69:31 and 75:25, whereas three phases were observed for the two solvent systems of ACE:MeOH=90:10 and 100:0 (Fig. 1b). A decrease in the drying rate and significant extended drying time were observed when polymer and celecoxib were added to the solvent systems (compare Fig. 1a, b).

Physicochemical Properties of Celecoxib-Loaded PLGA Microparticles

Celecoxib-loaded PLGA microparticles were prepared with the four different solvent systems, but at identical formulation and processing conditions. The estimation of the solubility of the polymer and celecoxib in ACE and MeOH is listed in Table I, and the physicochemical properties of the various microparticles are presented in Table II. For all four formulation types, the entrapment efficiency was around 100% and the residual moisture content was below 1% (Table II), despite the gentle spray-drying conditions. The microparticles were spherical with smooth surfaces and relatively narrow size distributions for all the four samples (Table II and Fig. 2). D_{50} of 1.63–2.8 μm and sizes distributions with Span in the range of 1.62–1.98 were observed for all samples prepared with the different solvent systems. The microparticles prepared at a high MeOH ratio (ACE: MeOH = 69:31) were smaller than those prepared at low MeOH ratios or in the absence of MeOH. As observed from the FIB-SEM images, the microparticles produced at high MeOH molar ratios exhibited a more compact inner structure, as compared to the microparticles prepared with solvents of a low MeOH molar ratio (Fig. 3). In addition, porous particles were observed in the samples prepared using 100% ACE and ACE:MeOH = 90:10.

Characterization of the Physical Solid State of Celecoxib-Loaded PLGA Microparticles

All spray-dried celecoxib-loaded PLGA microparticles formulations showed one endothermic event at approximately 46°C (Fig. 4a) (onset of the peak), which corresponds to the glass transition temperature of PLGA when analyzed by DSC. No melting events of celecoxib were observed in the thermograms of the microparticles, suggesting that the celecoxib was dispersed in the PLGA matrix as an amorphous state. This was supported by XRPD data, for which no crystalline diffraction was observed for the spray-dried microparticles (Fig. 4b). All spray-dried microparticles formulations exhibited a halo shape characteristic for the amorphous state.

Table I Physical Properties of Acetone and Methanol and Solubility of Celecoxib and PLGA in the Solvents

Solutes and physical properties of solvents	Acetone	Methanol
Solubility of celecoxib (%w/v)	60–70	10
Solubility of PLGA (%w/v)	50–60	Insoluble
Boiling point (°C)	56.0	64.0

Surface Chemical Analysis by XPS

The relative theoretical atomic concentration (in %) of C, O, F, N and S (H was not measured) of pure celecoxib were 65.38%, 7.69%, 11.54%, 11.54% and 3.85%, respectively. Similarly, the relative theoretical atomic concentration (in %) of C and O for PLGA were 55.56% and 44.44%, respectively. The concentration of celecoxib can be estimated directly from the atomic concentration of F, N and S atoms. In order to eliminate the errors, the ratios of N/F, S/F and F/C were used to calculate the celecoxib concentration at the surface of the microparticles, which was measured to be in the range of 10–22% (Table III), and there was a trend that this concentration increased significantly with an increase in the amount of MeOH in the feed solution.

Drug Release Behavior *in Vitro*

The *in vitro* drug release behavior of the celecoxib-loaded PLGA microparticles showed sustained release profiles (Fig. 5). In addition, the four different types of spray-dried microparticle formulations prepared at different solvent compositions exhibited different celecoxib release profiles. The microparticles prepared using ACE:MeOH = 69:31 showed a burst release of 50% of the drug within the initial 30 min, followed by a sustained release. The other three microparticles formulations showed diffusion-driven release profiles without a distinct burst release, and higher release rates were generally observed when the MeOH:ACE molar ratio was increased.

DISCUSSION

Effects of Solvent Power and Volatility on the Formation of PLGA Microparticles in the Spray-Drying Process

The formation of the particles in the spray-drying process is influenced by the physicochemical properties of the solvent, such as the volatility, polarity and solvent power to solutes. These factors determine the mass and heat transfer of the droplets after atomization of the feed solution, which in turn influence the characteristics of the particles resulting from the spray-drying process. The drying kinetics, as well as the interplay between the solute and solvent molecules, is critical determinants for the particle formation process. In the present study, the effects of drying rate and solvent power on the formation of PLGA microparticles during the spray-drying process were studied by varying systematically the composition of the solvent systems consisting of binary mixtures of ACE and MeOH. However, it is almost impossible

Table II Composition and Viscosity of Feed Solutions, and Physicochemical Properties of Celecoxib-Loaded PLGA Microparticles (5% (w/v) Solid Conc., 10% (w/w) Drug Content)

Feed solution		Characterization of the microparticles					
Composition (acetone: methanol molar ratio)	[η] (dL/g)	D_{10} (μm)	D_{50} (μm)	D_{90} (μm)	Span	EE (%)	RM (%)
69 : 31	0.154	0.68	1.63	3.90	1.98	101.4 ± 0.1	0.55 ± 0.06
75 : 25	0.188	0.96	2.17	4.89	1.81	102.7 ± 0.9	0.47 ± 0.05
90 : 10	0.204	1.34	2.80	5.88	1.62	106.9 ± 1.5	0.53 ± 0.03
100 : 0	0.236	1.08	2.46	5.65	1.86	106.4 ± 1.0	0.52 ± 0.07

Results denote mean ± SD (n=3)

to measure directly the drying rates in spray-drying processes due to the instantaneous evaporation of the solvent(s). Therefore, model systems are often used to study the drying kinetics. Here, we studied the drying kinetics of different solvent systems by measuring the evaporation rates of the solvents as a function of time, by monitoring the weight loss of the solvents and feed solutions using TGA under controlled temperature, surface area and nitrogen flow (31,36).

For the solvent systems without solutes, prolonged evaporation profiles were observed with an increase in the proportion of MeOH in the solvent systems (Fig. 1a), indicating that the higher the proportion of MeOH in the solvent system, the slower the drying rate. This can be attributed to the lower volatility of MeOH, as compared to ACE. Similar results have been reported for studies of the drying kinetics of binary solvent systems, which have shown that the evaporation coefficient of the solvent systems change as a function of time at constant drying conditions (37,38). During the last part of the drying process, the evaporation coefficient approaches the coefficient for the solvent with the lowest volatility (38,39).

The drying profiles of the feed solutions exhibited reduced evaporation rates, as compared to the solvent systems without solutes (Fig. 1a, b). As both drying kinetics studies were conducted at identical operation conditions, the prolonged drying profiles in the feed solutions can be attributed to the affinity between the solvent molecules and the polymer molecules, which reduced the rate of solvent evaporation. The decrease in the evaporation rate of the four different feed solutions can be attributed to the increased viscosity of the feed solutions at higher concentrations upon evaporation of the solvent because the molecular mobility is hindered.

The drying profiles of ACE:MeOH = 90:10 and ACE:MeOH = 100:0 were similar during the first drying phase, while in the second drying phase, ACE:MeOH = 90:10 showed a delayed drying profile (Fig. 1b). This indicates that the addition of a solvent with lower volatility (MeOH)

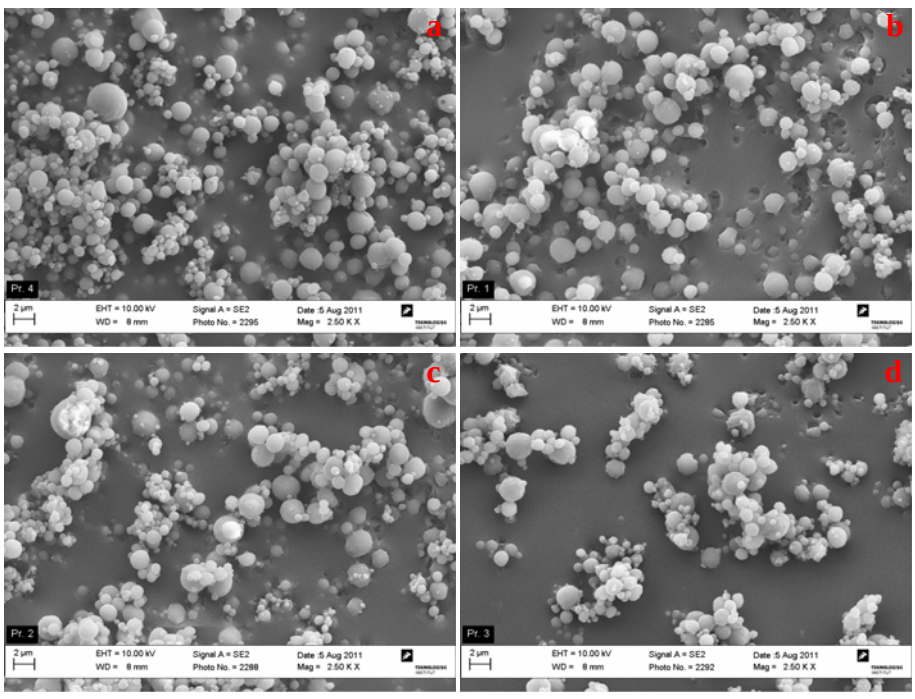

Fig. 2 SEM images of PLGA microparticles loaded with 10% (w/w) celecoxib prepared using the following binary solvent mixtures: ACE:MeOH = 69:31 (**a**), ACE:MeOH = 75:25 (**b**), ACE:MeOH = 90:10 (**c**) and ACE:MeOH = 100:0 (**d**).

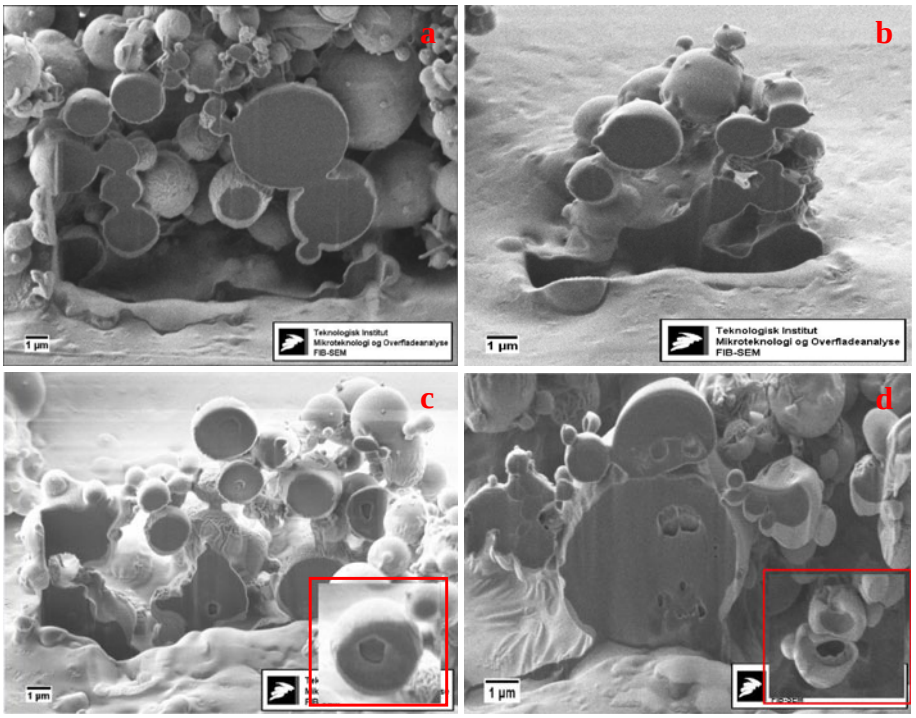

Fig. 3 FIB-SEM images of PLGA microparticles loaded with 10% (w/w) celecoxib prepared using the following binary solvent mixtures: ACE:MeOH=69:31 (**a**), ACE:MeOH=75:25 (**b**), ACE:MeOH=90:10 (**c**), ACE:MeOH=100:0 (**d**).

extends the drying time of the feed solution. However, no obvious extension of the drying time was found with an increase in the proportion of MeOH in the feed solutions from 10% (90:10 molar ratio) to 31% (69:31 molar ratio), even thought this was observed in the solvent systems (Fig. 1a). This suggests that the decrease in the viscosity of the polymer solutions with an increase in the content of MeOH may compensate for the reduced evaporation rates of the solutions containing higher amount of the solvent with low volatility.

At the early stage of the evaporation process, the ACE:MeOH = 75:25 and ACE:MeOH = 69:31 feed solutions

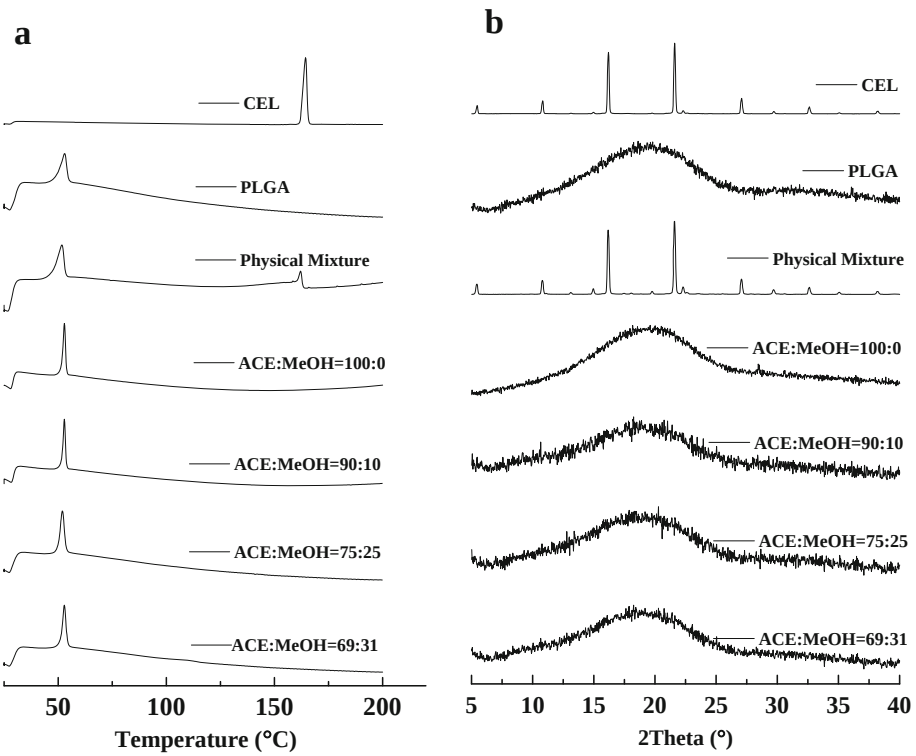

Fig. 4 Representative DSC thermograms (**a**) and representative XRPD profiles (**b**) of celecoxib, PLGA, physical mixture of celecoxib and PLGA, and PLGA microparticles loaded with 10% (w/w) celecoxib prepared using different solvent systems.

Table III Chemical Surface Composition of Celecoxib-Loaded PLGA Microparticles (5% (w/v) Solid Conc., 10% (w/w) Drug Content)

Composition of feed solution	Elemental analysis			
Acetone:methanol molar ratio	N/F	S/F	F/C	Conc. of Celecoxib
69 : 31	0.96 ± 0.07	0.39 ± 0.09	0.040 ± 0.001	22 ± 1%*
75 : 25	0.35 ± 0.07	0.13 ± 0.03	0.047 ± 0.006	18 ± 7%
90 : 10	0.89 ± 0.04	0.34 ± 0.02	0.018 ± 0.001	10 ± 1%*
100 : 0	0.96 ± 0.15	–	0.026 ± 0.003	14 ± 2%

Results denote mean ± SD (n=3). Results significantly different from microparticles prepared with acetone are indicated: * $p < 0.05$

exhibited two-step drying profiles, i.e. a rapid decrease in the evaporation rate (5–15 min), followed by a slow decrease in the evaporation rate (15–40 min), while the ACE:MeOH = 90:10 feed solution exhibited a linear reduction in the evaporation rate between 5 and 40 min, which is similar to the ACE:MeOH = 100:0 feed solution. This indicates that addition of MeOH to the solvent system alters the drying kinetics of the feed solution. Because MeOH is a poor solvent for PLGA, an anti-solvent precipitation of the polymer may occur when the molar ratio between ACE and MeOH decreases upon evaporation due to the higher volatility of ACE, as compared to MeOH. On the other hand, anti-solvent precipitation of celecoxib is unlikely to occur as it can be dissolved in both ACE and MeOH, and the concentration of celecoxib in the feed solution is rather lower, as compared to the PLGA concentration. Considering the difference in molecular weight of celecoxib and PLGA, and the mass transfer involved in the spray-drying process, a different migration rate of celecoxib and PLGA can be expected during the solidification of the droplets, eventually influencing the distribution of the two molecules in the resulting microparticles.

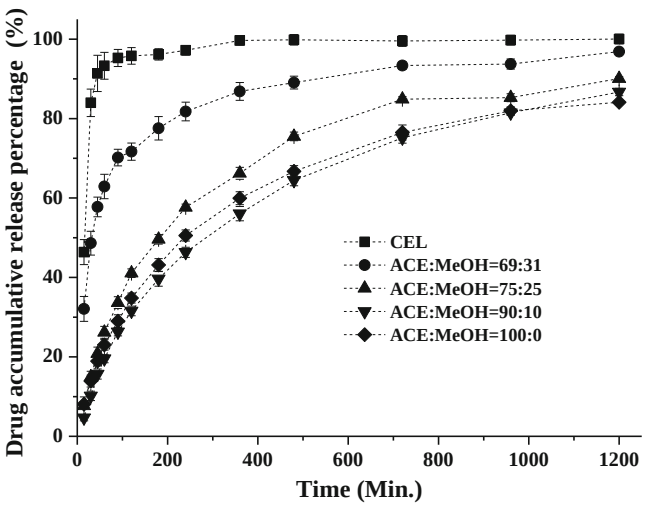

Fig. 5 *In vitro* drug release profiles of PLGA microparticles loaded with 10% (w/w) celecoxib prepared using different solvent systems. Results denote mean ± SD (*n*=4).

Effect of Solvent Power and Volatility on the Physicochemical Properties and Release Profiles of Celecoxib-Loaded PLGA Microparticles

Varying the solvent composition did not significantly influence the encapsulation efficiency, residual moisture content and morphology of the PLGA microparticles in the current study (Fig. 2 and Table II). As expected, the encapsulation efficiency of celecoxib was about 100%, regardless of the solvent composition. The low residual moisture content in the microparticles suggests that the process parameters used in the present study are appropriate for effective drying of the PLGA microparticles, even though different solvent compositions were used. Furthermore, applying an outlet temperature below the T_g of PLGA effectively prevented agglomeration of the PLGA microparticles. All four microparticle-based formulations exhibited a similar spherical shape, and no fusion of the microparticles was observed.

The particle size of the spray-dried microparticles appeared to be dependent on the solvent composition. The microparticles tended to become smaller with an increase in the proportion of MeOH in the solvent systems. This can be attributed to the fact that the viscosity of the PLGA solution is decreased (See Table II) when MeOH (a poor solvent) is added to ACE (a good solvent). The decrease in the viscosity of the PLGA solution resulted in a decreased size of the atomized droplets and therefore also a smaller size of the dry particles (40), indicating that the solvent power can influence the size of the polymeric microparticles produced by spray-drying by altering the viscosity of the feed solution. Furthermore, the drying rate of the solvent systems was decreased by increasing the ratio of MeOH to ACE (Fig. 1a), which caused a prolonged solidification time for the PLGA microspheres and shrinkage, resulting in a smaller particle size and the formation of a compact inner structure. This finding is supported by FIB-SEM studies of the microparticles (see Fig. 2).

The majority of the PLGA microparticles has a condensed texture. This can be attributed to the relatively high solid concentrations and the mild drying conditions applied in this study. Nevertheless, some porous particles were found in the samples prepared with 100% ACE and ACE:

MeOH = 90:10, while this was not the case for the samples prepared with ACE:MeOH = 75:25 and ACE:MeOH = 69:31 (see Fig. 2). This can be explained by the distinct evaporation rates of the different solvents compositions. The faster evaporation rate of pure ACE or ACE:MeOH = 90:10 results in less time for the droplets to shrink due to the early formation of the shell, as compared to the droplets in ACE:MeOH = 75:25 and ACE:MeOH = 69:31 systems.

Other studies on the effect of solvent composition on the miscibility and physical stability of solid dispersions (31,36) have showed that application of a mixture of a good solvent and an anti-solvent with more narrow volatility difference results in solid dispersions with better miscibility and physical stability. In the present study, the different solvent compositions used in this study did not result in detectable differences in the solid state properties of celecoxib in the PLGA matrix, even though the evaporation rate of the solvent systems was shown to be different in the TGA study. This may be due to the instant evaporation of the solvents in the spray-drying process and to the high ratio between polymer and celecoxib. Celecoxib was appeared to be molecularly dispersed in the PLGA matrix after the spray-drying process, which was supported by both DSC and XRPD studies (Fig. 4). However, applying different solvent compositions resulted in different surface chemistry of the microparticles. As shown in the surface analysis using XPS, a high surface enrichment of celecoxib was observed upon increasing the proportion of MeOH in the solvent system (Table III). This can be explained by the different migration rate of celecoxib and PLGA during the particle formation process. For example, in the co-solvent systems of ACE:MeOH = 75:25 and ACE:MeOH = 69:31, anti-solvent precipitation of PLGA might occur prior to the precipitation of celecoxib due to the better solubility of celecoxib than PLGA in both MeOH and ACE. The celecoxib molecules might thus migrate to the particle surface during diffusion of the residual solvents (i.e. ACE and MeOH) from the inner core towards the outer shell of the particles, eventually resulting in the surface enrichment of celecoxib.

The drug release behavior from PLGA matrices can be diffusion-driven or diffusion-driven followed by erosion-driven release due to hydrolysis of the PLGA ester bond linkages (33). For the uncapped PLGA used in this study, a visible erosion of the PLGA matrix has been reported to take place after at least 15 days, depending also on the size and texture of the particles (33). In the present study, the release rates of celecoxib-loaded PLGA microparticles were investigated in aqueous solutions containing SDS for 20 h. Thus, the drug release behavior was most likely diffusion-driven and influenced mainly by the PLGA network and the radial distribution of the drug in the microparticles.

As shown in the release study, the release rates of celecoxib from the microparticles were found to be different, even though the formulation compositions in the microparticles were identical. This could be attributed to the different physicochemical properties of the particles resulting from the spray-drying process when using different solvent compositions. As expected, a burst release was found for the microparticles produced with the solvent composition of ACE:MeOH = 69:31 (Fig. 5), which has the highest surface enrichment of celecoxib and smallest particle size. Moreover, considering the celecoxib surface enrichment of the microparticles prepared using ACE:MeOH = 69:31 was just about 22%, while the burst release in the initial 15 min was more than 30%, which was higher than the drug surface enrichment; while, the burst release during the initial 15 min for the other three samples was around 7–8%, which were less than the drug surface enrichment (10–18%). This suggests that the release of celecoxib from the PLGA microparticles is not only influenced by the physical properties of the microparticles (such as the surface enrichment, size, density, etc.), but also the structure state of the PLGA matrix, which is determined by the conformational structure of PLGA in the microparticles and the network of the polymer molecules. It is because the conformational structures of PLGA in the solvent systems can vary depending on the proportion of good solvent and poor solvent in the systems, which were reflected by the different rheological parameters (such as viscosity in Table II). The instant precipitation of PLGA from the different solvent systems in the spray-drying process may result in different conformational structures of PLGA in the microparticles and different networks in the microparticles, which could affect the celecoxib release profiles.

CONCLUSION

This study elucidated the influence of solvent power and volatility on the particle formation process and the physicochemical properties of PLGA microparticles produced *via* the spray-drying process. Even for the identical formulations, the physical properties of the particles, such as the particle size and texture can be adjusted by varying the solvent composition. Owing to the differences in the molecular weight and solubility of the solutes in the given solvent mixtures, the drug and polymer molecules exhibited different diffusion rates during the process of particle formation, resulting in a non-homogenous drug distribution in the resulting particles. This was demonstrated by the surface enrichment of the drug when varying the solvent compositions. The drug release profiles of the microparticles were dependent on the solvent composition. It is because different solvent compositions might result in not only varied physical properties of the particles but also different network and conformational structure of the polymers in the particles.

The present study highlights the complexity of the process of particle formation *via* spray-drying and the potential for rational particle engineering *via* understanding of the interplay between formulation and solvent components during spray-drying.

ACKNOWLEDGMENTS AND DISCLOSURES

This work was funded by The Danish Council for Technology and Innovation *via* the Innovation Consortium NanoMorph (952320/2009), The Drug Research Academy and The Danish Agency for Science, Technology and Innovation. The authors would also like to thank Erik Wisaeus, Kenneth Brian Haugshøj and Pia Wahlberg (Danish Technological Institute) and Dorthe Ørbæk (Faculty of Health and Medical Sciences, University of Copenhagen) for technical assistance with the SEM, FIB-SEM, XPS and TGA analysis.

REFERENCES

1. Vehring R. Pharmaceutical particle engineering *via* spray drying. Pharm Res. 2008;25:999–1022.
2. Delie F, Blanco-Prieto MJ. Polymeric particles to improve oral bioavailability of peptide drugs. Molecules. 2005;10:65–80.
3. Cook RO, Pannu RK, Kellaway IW. Novel sustained release microspheres for pulmonary drug delivery. J Control Release. 2005;104:79–90.
4. Alhalaweh A, Andersson S, Velaga SP. Preparation of zolmitriptan–chitosan microparticles by spray drying for nasal delivery. Eur J Pharm Sci. 2009;38:206–14.
5. Kristen Bowey RJN. Systemic and mucosal delivery of drugs within polymeric microparticles produced by spray drying. BioDrugs. 2010;24:359–77.
6. Fude C, Dongmei C, Anjin T, Mingshi Y, Kai S, Min Z, *et al.* Preparation and characterization of melittin-loaded poly (dl-lactic acid) or poly (dl-lactic-co-glycolic acid) microspheres made by the double emulsion method. J Control Release. 2005;107:310–9.
7. Yang M, Cui F, You B, You J, Wang L, Zhang L, *et al.* A novel pH-dependent gradient-release delivery system for nitrendipine. J Control Release. 2004;98:219–29.
8. Chow AH, Tong HH, Chattopadhyay P, Shekunov BY. Particle engineering for pulmonary drug delivery. Pharm Res. 2007;24:411–37.
9. Shoyele SA, Cawthorne S. Particle engineering techniques for inhaled biopharmaceuticals. Adv Drug Deliv Rev. 2006;58:1009–29.
10. Kwok PC, Tunsirikongkon A, Glover W, Chan HK. Formation of protein nano-matrix particles with controlled surface architecture for respiratory drug delivery. Pharm Res. 2011;28:788–96.
11. Iskandar F, Nandiyanto ABD, Widiyastuti W, Young LS, Okuyama K, Gradon L. Production of morphology-controllable porous hyaluronic acid particles using a spray-drying method. Acta Biomater. 2009;5:1027–34.
12. Tsapis N, Bennett D, Jackson B, Weitz DA, Edwards DA. Trojan particles: large porous carriers of nanoparticles for drug delivery. Proc Natl Acad Sci U S A. 2002;99:12001–5.
13. Maa YFPS. Biopharmaceutical powders particle formation and formulation considerations. Curr Pharm Biotechnol. 2000;1:283–302.
14. Saluja V, Amorij JP, Kapteyn JC, de Boer AH, Frijlink HW, Hinrichs WL. A comparison between spray drying and spray freeze drying to produce an influenza subunit vaccine powder for inhalation. J Control Release. 2010;144:127–33.
15. Mohri K, Okuda T, Mori A, Danjo K, Okamoto H. Optimized pulmonary gene transfection in mice by spray-freeze dried powder inhalation. J Control Release. 2010;144:221–6.
16. Bi R, Shao W, Wang Q, Zhang N. Spray-freeze-dried dry powder inhalation of insulin-loaded liposomes for enhanced pulmonary delivery. J Drug Target. 2008;16:639–48.
17. Casettari L, Castagnino E, Stolnik S, Lewis A, Howdle SM, Illum L. Surface characterisation of bioadhesive PLGA/chitosan microparticles produced by supercritical fluid technology. Pharm Res. 2011;28:1668–82.
18. Salmaso S, Elvassore N, Bertucco A, Caliceti P. Production of solid lipid submicron particles for protein delivery using a novel supercritical gas-assisted melting atomization process. J Pharm Sci. 2009;98:640–50.
19. Lee YH, Mei F, Bai MY, Zhao S, Chen DR. Release profile characteristics of biodegradable-polymer-coated drug particles fabricated by dual-capillary electrospray. J Control Release. 2010;145:58–65.
20. Jaworek A. Micro- and nanoparticle production by electrospraying. Powder Technol. 2007;176:18–35.
21. Jaworek A, Sobczyk AT. Electrospraying route to nanotechnology: an overview. J Electrost. 2008;66:197–219.
22. Ogain ON, Li J, Tajber L, Corrigan OI, Healy AM. Particle engineering of materials for oral inhalation by dry powder inhalers. I-Particles of sugar excipients (trehalose and raffinose) for protein delivery. Int J Pharm. 2011;405:23–35.
23. Rizi K, Green RJ, Donaldson M, Williams AC. Production of pH-responsive microparticles by spray drying: investigation of experimental parameter effects on morphological and release properties. J Pharm Sci. 2011;100:566–79.
24. Baldinger A, Clerdent L, Rantanen J, Yang M, Grohganz H. Quality by design approach in the optimization of the spray-drying process. Pharm Dev Technol. 2011.
25. Maltesen MJ, Bjerregaard S, Hovgaard L, Havelund S, van de Weert M. Quality by design—spray drying of insulin intended for inhalation. Eur J Pharm Sci. 2008;70:828–38.
26. Rabbani NR, Seville PC. The influence of formulation components on the aerosolisation properties of spray-dried powders. J Control Release. 2005;110:130–40.
27. Vehring R, Foss W, Lechugaballesteros D. Particle formation in spray drying. J Aerosol Sci. 2007;38:728–46.
28. Feng AL, Boraey MA, Gwin MA, Finlay PR, Kuehl PJ, Vehring R. Mechanistic models facilitate efficient development of leucine containing microparticles for pulmonary drug delivery. Int J Pharm. 2011;409:156–63.
29. Ivey JW, Vehring R. The use of modeling in spray drying of emulsions and suspensions accelerates formulation and process development. Comput Chem Eng. 2010;34:1036–40.
30. Mezhericher M, Levy A, Borde I. Spray drying modelling based on advanced droplet drying kinetics. Chem Eng Process. 2010;49:1205–13.
31. Paudel A, Mooter G. Influence of solvent composition on the miscibility and physical stability of naproxen/PVP K 25 solid dispersions prepared by cosolvent spray-drying. Pharm Res. 2012;29:251–70.
32. Wang F-J, Wang C-H. Sustained release of etanidazole from prepared by non- spray dried microspheres halogenated solvents. J Control Release. 2002;81:263–80.

33. Giteau A, Venier-Julienne MC, Aubert-Pouëssel A, Benoit JP. How to achieve sustained and complete protein release from PLGA-based microparticles? Int J Pharm. 2008;350:14–26.
34. Chawla G, Gupta P, Thilagavathi R, Chakraborti AK, Bansal AK. Characterization of solid-state forms of celecoxib. Eur J Pharm Sci. 2003;20:305–17.
35. Mu L, Teo M-M, Ning H-Z, Tan C-S, Feng S-S. Novel powder formulations for controlled delivery of poorly soluble anticancer drug: application and investigation of TPGS and PEG in spray-dried particulate system. J Control Release. 2005;103:565–75.
36. Wu JX, Yang M, Berg F, Pajander J, Rades T, Rantanen J. Influence of solvent evaporation rate and formulation factors on solid dispersion physical stability. Eur J Pharm Sci. 2011;44:610–20.
37. Yarin AL, Brenn G, Rensink D. Evaporation of acoustically levitated droplets of binary liquid mixtures. Int J Heat Fluid Flow. 2002;23:471–86.
38. Schiffter HA. Single droplet drying of proteins and protein formulations *via* acoustic levitation. PhD Thesis Friedrich-Alexander-University, Erlangen, Germany.
39. Wulsten E, Kiekens F, van Dycke F, Voorspoels J, Lee G. Levitated single-droplet drying: case study with itraconazole dried in binary organic solvent mixtures. Int J Pharm. 2009;378:116–21.
40. Shenoy S, Bates W, Frisch H, Wnek G. Role of chain entanglements on fiber formation during electrospinning of polymer solutions: good solvent, non-specific polymer-polymer interaction limit. Polymer. 2005;46:3372–84.